

# Prediction of soil properties by digital terrain modelling

I.V. Florinsky<sup>a, b, \*</sup>, R.G. Eilers<sup>c</sup>, G.R. Manning<sup>a</sup>, L.G. Fuller<sup>d</sup>

<sup>a</sup> Department of Soil Science, University of Manitoba, 362 Ellis Building, Winnipeg, Manitoba, Canada R3T 2N2

<sup>b</sup> Institute of Mathematical Problems of Biology, Russian Academy of Sciences, Pushchino, Moscow Region, 142292, Russia

<sup>c</sup> Land Resource Unit, Agriculture and Agri-Food Canada, 360 Ellis Building, University of Manitoba, Winnipeg, Manitoba, Canada R3T 2N2

<sup>d</sup> Department of Renewable Resources, University of Alberta, 731 General Services Building, Edmonton, Alberta, Canada T6G 2H1

Received 6 April 2000; received in revised form 10 August 2000; accepted 29 July 2001

## Abstract

We investigated two approaches for large-scale analysis and prediction of the spatial distribution of soil properties in an agricultural landscape in the Canadian prairies. The first approach was based on the implementation of nine types of digital terrain models (DTMs) and regression analysis of soil and topographic data. The second approach used a concept of accumulation, transit, and dissipation zones of the landsurface. Soil properties were soil moisture, residual phosphorus, solum thickness, depth to calcium carbonate, and organic carbon content. The dependence of soil properties on topography was supported by correlations for the upper soil layer. However, topographic control of soil moisture and residual phosphorus decreased with depth. Also, correlation coefficients and regression equations describing topographic control of soil moisture and residual phosphorus differed among seasons. This imposes limitations on regression-based predictions of the spatial distribution of soil properties. The prediction of soil property distribution with the concept of accumulation, transit and dissipation zones can be more successful and appropriate than the prediction based on linear regression. The variability in relationships between soil and topographic characteristics with depth may stem from spatial variability in the rate of decline of hydraulic conductivity with depth. Temporal variability in soil–topography relationships occurs because soil properties result from interactions of a variety of pedogenetic factors and processes marked by different temporal variability. In soil studies with digital terrain modelling, there is a need to take into account four types of variability in relations between soil and relief: regional, temporal, depth, and scale. © 2002 Elsevier Science Ltd. All rights reserved.

**Keywords:** Digital terrain model; Topography; Prediction map; Soil; Statistical analysis

## Software availability

Name of the software: LANDLORD

Developer: I.V. Florinsky, T.I. Grokhlina, P.V. Kozlov, G.L. Andrienko, N.V. Andrienko, and N.L. Mikhailova, Institute of Mathematical Problems of Biology, Russian Academy of Sciences, Pushchino, Moscow Region, 142292, Russia.  
Email: florinskyi@em.agr.ca

Year first available: 1993

Hardware required: PC 486dx, 16 Mb RAM

Software required: MS Windows 3.xx, 95, 98

Program language: Borland C, Borland C++, Borland Delphi

Program size: 2378 kb

Availability and cost: Available at a cost of US\$ 2000

## 1. Introduction

Analysis and forecast of the spatial distribution and dynamics of soil properties is an important element of sustainable land management. Topography is one of the pedogenetic state factors identified by many soil scientists (Dokuchaev, 1892; Jenny, 1961; Huggett, 1975; Gerrard, 1981). Thus, quantitative information on relief is often used in soil studies including the modelling and prediction of soil properties (Pennock et al., 1987; Moore et al., 1993; Beven et al., 1995).

Quantitative topographic data have been used in the form of digital terrain models (DTMs) for the past two decades. DTMs are digital representations of variables describing the topographic surface, such as digital elevation models (DEMs) and models of the variables listed in Table 1 (Burrough, 1986; Shary, 1995). Digital terrain modelling is a system of quantitative methods to analyse and model the landsurface and relationships between the

\* Corresponding author. Tel.: +1-204-474-6120; fax: +1-204-474-7633.

E-mail address: florinskyi@em.agr.ca (I.V. Florinsky).

Table 1

Definitions, formula and physical interpretations of some topographic variables (Speight, 1968; Beven and Kirkby, 1979; Moore et al., 1991; Shary, 1991; Florinsky and Kuryakova, 1996; MacMillan and Pettapiece, 1997)

Variable	Definition and formula	Interpretation
Slope gradient ( $G$ ), °	An angle between a tangent plane and a horizontal one at a given point on the landsurface: $G = \arctan \sqrt{p^2 + q^2}$ <sup>a</sup>	Velocity of substance flows
Slope aspect ( $A$ ), °	An angle clockwise from north to a projection of an external normal vector to a horizontal plane at a given point on the landsurface: $A = \arctan \left( \frac{q}{p} \right)$ <sup>a</sup>	Direction of substance flows
Vertical curvature ( $k_v$ ), $m^{-1}$	A curvature of a normal section of the landsurface by a plane, including gravity acceleration vector at a given point: $k_v = -\frac{p^2 r + 2pq s + q^2 t}{(p^2 + q^2) \sqrt{(1 + p^2 + q^2)^3}}$ <sup>a</sup>	Relative deceleration of substance flows
Horizontal curvature ( $k_h$ ), $m^{-1}$	A curvature of a normal section of the landsurface. This section is orthogonal to the section of vertical curvature at a given point on the landsurface: $k_h = -\frac{q^2 r - 2pq s + p^2 t}{(p^2 + q^2) \sqrt{1 + p^2 + q^2}}$ <sup>a</sup>	Convergence of substance flows
Mean curvature ( $H$ ), $m^{-1}$	$H = (k_h + k_v) / 2$	Flow convergence and relative deceleration with equal weights
Accumulation curvature ( $K_a$ ), $m^{-2}$	$K_a = k_h \cdot k_v$	Degree of flow accumulation
Specific catchment area (CA), $m^2 m^{-1}$	A ratio of an area of an exclusive figure formed on the one hand by a contour intercept with a given point on the landsurface and, on the other by flow lines coming from the upslope to the ends of this contour intercept, to the length of this intercept	Contributing area
Topographic index (TI)	$TI = \ln(CA/G)$	Extent of flow accumulation
Stream power index (SI)	$SI = CA \cdot G$	Extent of potential flow erosion
Relative relief (RR), %	A ratio of the difference in elevations between a given point on the landsurface and the lowest point of a watershed to the difference in elevations between the highest and the lowest points of a watershed	Landscape drainage characteristic

<sup>a</sup>  $r, t, s, p$  and  $q$  are partial derivatives of the function  $z=f(x,y)$ :  $r = \frac{\delta^2 z}{\delta x^2}$ ,  $t = \frac{\delta^2 z}{\delta y^2}$ ,  $s = \frac{\delta^2 z}{\delta x \delta y}$ ,  $p = \frac{\delta z}{\delta x}$  and  $q = \frac{\delta z}{\delta y}$ . Moving the 3×3 elevation submatrix along a regular DEM, we can calculate values of  $r, t, s, p$  and  $q$  for all points of the DEM, except boundary points (Evans, 1980; Moore et al., 1993; Shary, 1995).

topography and geological, hydrological, biological and anthropogenic components of the landscape. Digital terrain modelling is used increasingly to solve a wide range of geoscientific problems (Moore et al., 1991; Shary et al., 1991; Weibel and Heller, 1991; Florinsky, 1998).

Most DTM-based predictions of soil properties are built upon statistical models describing relationships between soil and topographic attributes at each point of a landscape (Moore et al., 1993; Bell et al., 1994; Odeh et al., 1994; Gessler et al., 1995; Thompson et al., 1997; Arrouays et al., 1998). However, correct prediction of a soil property at each landscape point is difficult because of the high spatial variability of soil properties (Burrough, 1993). Also, sometimes there is a need to know mean values of a soil property within typical topographic features (e.g. crest, midslope and depression) and not the value of a soil property at each point in a landscape.

For example, Fedoseev (1959) used (a) a coefficient describing the water storage in the root zone for different landforms relative to a reference hillslope, and (b) data on the seasonal dynamics of soil moisture depending on slope gradient ( $G$ ), aspect ( $A$ ) (Table 1) and a type of slope shape (convex, concave and flat) to predict the spatial distribution of soil moisture. Romanova (1970, 1971) developed methods for predictive mapping of seasonal moisture distribution with terrain segmentation by values of  $G$ ,  $A$ , and a type of slope shape, and derived empirical graphs describing the dependence of soil moisture on these attributes. Stepanov et al. (1984) performed terrain segmentation using a criterion of sign of horizontal curvature ( $k_h$ ) (positive or negative) for large-, middle- and small-scale soil mapping. Closely related methods of terrain segmentation by  $k_h$  and vertical curvature ( $k_v$ ) signs and  $G$  values were applied to analyse soil profile morphology (Pennock et al., 1987) and to compile middle-scale soil maps (Satalkin, 1996). MacMillan and Pettapiece (1997) used a similar technique to predict soil spatial distribution using  $G$  and relative relief (RR) (Table 1) as deciding factors.

However, correct identification of topographic features can be difficult with such approaches to landscape segmentation. Authors cited have used subjective segmentation criteria, such as empirical threshold values of  $G$  and RR. This is because there are no rigorous quantitative definitions for qualitative geomorphic concepts of 'crest', 'midslope', and 'depression'. We suppose that a more appropriate alternative is to segment a landscape into polygons with a concept of accumulation, transit and dissipation zones (Shary et al., 1991; Florinsky, 2000), since these quantitative terms may express the qualitative geomorphic notions of depression, midslope and crest, respectively (Section 3.4).

Apart from the high spatial variability of soil properties, two other poorly explored factors can essentially influence accuracy of DTM-based soil predictions. First,

there is a temporal variability in soil–topography relationships. Long-term observations of soil moisture dynamics have been used to compile generalised tables and diagrams of possible values of soil moisture among slopes with different  $G$ ,  $A$  and shape in different seasons and in various climates (Taychinov and Fayzullin, 1958; Fedoseev, 1959; Romanova, 1977). Burt and Butcher (1985) described the temporal variability in the dependence of saturation depth and slope discharge on  $k_h$  and topographic index (TI), but there were no explanations of this phenomenon. Hedddadj and Gascuel-Oudou (1999) found seasonal variations in the dependence of unsaturated hydraulic conductivity on slope position, but they used a qualitative description of the relief.

Second, there is a variation in topographic control of soil properties with depth. It is essential to recognise an effective soil layer, wherein relations between soil and topography are observable and significant. For example, an assumption that soil moisture content decreases with depth due to a decline in hydraulic conductivity is used in TOPMODEL, a DTM-based soil-hydrological model (Beven and Kirkby, 1979; Beven et al., 1995). However, there are no hypotheses for varying the extent of topographic control on soil moisture with depth. It is apparent that variability in soil–topography relationships with depth and over time is critical to accuracy of DTM-based soil predictions.

In this paper, we studied two approaches for large-scale analysis and prediction of spatial distribution of soil properties in a low relief agricultural landscape in the Canadian prairies. The first used the application of nine types of DTMs and linear regression of soil and topographic data. The second used the concept of accumulation, transit, and dissipation zones. The comparison of the approaches was carried out with regard to the temporal variability in relations between soil and topographic attributes, and variations in the topographic influence on soil properties with increasing depth.

## 2. Study site

A study site is located approximately 280 km west of the city of Winnipeg, Manitoba, Canada, at the Miniota Precision Agriculture Research Site at Bell Farms (Fig. 1). The site measures 809 by 820 m with a difference in elevation of about 6 m (Fig. 2). It is situated in the Newdale Plain at an elevation of about 500 m above sea level. The site is representative of a broad region of undulating glacial till landscapes in the Western Canada (Clayton et al., 1977).

The site is located in a continental climate zone with warm summers and prolonged, cold winters. The mean summer temperature is 16°C, the mean winter temperature is –11°C. Mean annual precipitation is about 460 mm including 310 mm of rainfall and 150 mm of snowfall (Fitzmaurice et al., 1999).

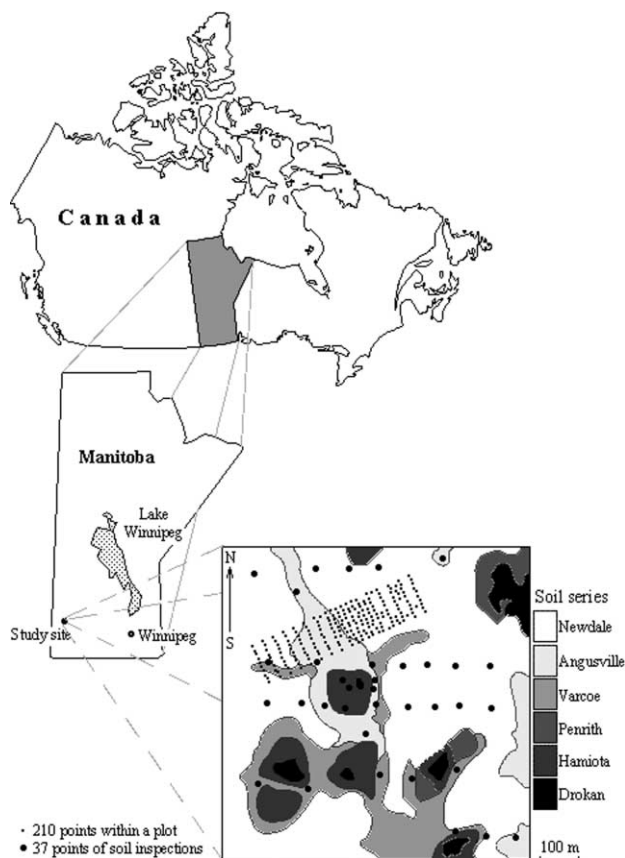


Fig. 1. Geographical position of the study site ( $50^{\circ}13'40''$  N,  $100^{\circ}51'20''$  W), soils series, and distribution of sampling points.

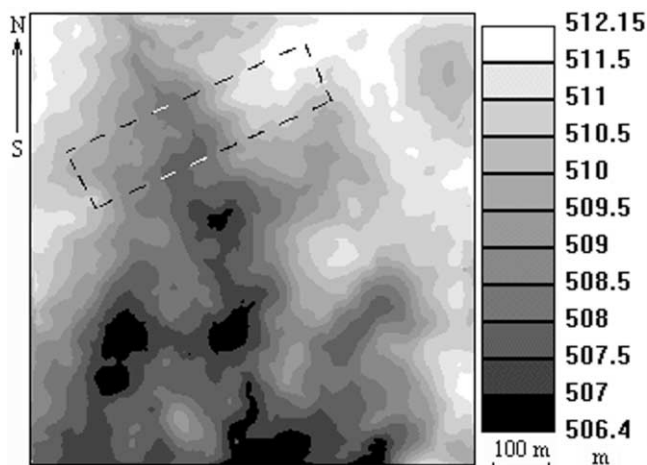


Fig. 2. The study site, elevations. Dashed lines indicate the plot.

The parent material consists of loamy textured glacial till deposits (Clayton et al., 1977). Soils at the site are Black Chernozems and Gleysols (Soil Classification Working Group, 1998). Orthic Black Chernozems (Newdale series) predominate on well-drained crests and midslopes. Imperfectly drained soils in the lower to toe slope positions are Gleyed Eluviated Black Chernozems (Angusville series). Minor areas of imperfectly drained

Gleyed Carbonated Rego Black Chernozems (Varcoe series) occur near the toe slopes in close association with Angusville soils. Gleysols (Penrith, Hamiota, and Drokan series) predominate in poorly drained depressions (Fig. 1 and Table 2) (Fitzmaurice et al., 1999).

There are no permanent streams within the site, but there is temporary ponding in some depressions in spring. Native vegetation of willows (*Salix sp.*), aspen (*Populus tremuloides*) and sedges (*Carex sp.*) surrounds depressions. Most of the site has been cropped for over 50 years. Before 1976, the field was farmed in a wheat-fallow rotation. In 1976, continuous cropping was initiated, with a cereal-broadleaf rotation. Since 1988, a zero-tillage management system has been employed.

### 3. Materials and methods

#### 3.1. Soil sampling

A plot was selected within the site to include a typical soil catena; it measures 450 by 150 m with a difference in elevation of 4.2 m (Fig. 2). The plot consisted of 10 adjacent and equally spaced 450 m transects with 21 sampling points in each of these transects, for a total of 210 sampling points in the plot (Fig. 1). Of the 21 points in each transect, there were 16 uniformly spaced sampling points on a basis of 30 m. Additional five points were interspersed at 15 m intervals between the original 16 points at areas of pronounced inflection in the slope shape. This design allowed us to describe variations of soil properties due to topographic influence within the catena. Each the 210 points were georeferenced with horizontal accuracy of 0.03 m by a global positioning system (GPS) receivers Trimble 4600LS Surveyors.

Soil was sampled for gravimetric moisture and residual phosphorus at the 210 points in four depth increments (0–0.3, 0.3–0.6, 0.6–0.9 and 0.9–1.2 m) using soil augers (Carter, 1993). Soil moisture was determined in each depth increment for six times: early May, early July and late August 1997 and 1998 (only 0–0.3 and 0.3–0.6 m increments were collected in August 1997). Samples for residual phosphorus content were obtained in early May 1997 and 1998. In September 1997, a truck-mounted hydraulic coring device was utilised to obtain intact 0.04 m diameter soil cores in polyethylene sleeves at the 210 points (Klute, 1986; Carter, 1993). These were used to evaluate solum thickness, depth to calcium carbonate, and organic carbon content of the A horizon at the 210 points.

Gravimetric soil moisture was determined by heating 20–30 g of moist soil at  $105^{\circ}\text{C}$  for 24 h (Klute, 1986; Carter, 1993). Residual phosphorus was extracted using ammonium acetate and analysed by automated molybdate colorimetry (Page et al., 1982; Carter, 1993). Organic carbon content of the A horizon was determined

Table 2  
Assessed values of some soil properties within the study site (Fitzmaurice et al., 1999)

Soil series	Horizon	Sand, %	Silt, %	Clay, %	pH	Hydraulic conductivity, mm h <sup>-1</sup>	Bulk density, g cm <sup>-3</sup>
Newdale	A <sub>p</sub>	30	36	34	7.2	3	0.99
	A <sub>h</sub>	42	30	28	7.1	1.3	1.42
	B <sub>m</sub>	34	35	31	7.3	3	1.53
	BC	35	34	31	7.6	3	1.6
	C <sub>k</sub>	38	36	26	7.9	1.95	1.63
Angusville	A <sub>p</sub>	40	40	20	6.7	3	1.25
	A <sub>hegj</sub>	35	45	20	7	3	1.56
	A <sub>egj</sub>	32	46	22	6.6	1.9	1.44
	BA	29	35	36	6.5	3	1.45
	B <sub>tgj</sub>	26	34	40	6.9	0.1	1.45
	BC	40	33	27	7.4	3	1.45
	C <sub>ca gj</sub>	31	44	25	7.7	1.95	1.55
	C <sub>kgj</sub>	38	36	26	7.9	1.95	1.63
Varcoe	A <sub>pk</sub>	26	38	36	8	3	1.04
	A <sub>hk</sub>	20	42	38	7.9	0.4	1.33
	AC	25	39	36	8	4	1.4
	C <sub>kg</sub>	18	44	38	8	1.95	1.4
Penrith	A <sub>p</sub>	25	60	15	6.7	3	1.5
	BA	33	35	32	6.8	0.3	1.42
	B <sub>tg</sub>	34	24	42	7.3	0.1	1.42
	BC	37	30	33	7.4	0.3	1.51
	C <sub>kg</sub>	38	36	26	7.9	1.95	1.63
Hamiota	LFH	0	0	0	6.5	3	0.15
	A <sub>h</sub>	15	47	38	6.5	0.3	1.3
	B <sub>g</sub>	35	26	39	7.3	0.1	1.4
	C <sub>cag</sub>	48	31	21	7.6	3	1.5
	C <sub>kg</sub>	38	35	27	7.6	1.95	1.5
Drokan	A <sub>hk</sub>	25	38	37	7.9	3	1.3
	AC	25	39	36	8	1.95	1.4
	C <sub>kg</sub>	18	44	38	7.8	1.95	1.5

(LFH — organic horizons characterised by an accumulation of organic matter in which the original structure is easily discernible (L), partly decomposed (F), and decomposed (H) organic matter. Lowercase suffixes: ca — horizon of secondary carbonate enrichment; e — horizon characterised by the eluviation of clay, Fe, Al, and organic matter; g — horizon characterised by grey colours and prominent mottling indicating permanent or periodic intense reduction; h — horizon enriched with organic matter; j — an expression of, but failure to meet, a specified limits of the suffix e, g and t; k — the presence of carbonate; m — evidence of removal of carbonates completely; p — horizon disturbed by cultivation; t — an illuvial horizon enriched with silicate clay (Soil Classification Working Group, 1998))

by dry combustion of 0.12 g of oven-dried soil with a Leco CHN 600 C and N analyser (Page et al., 1982; Carter, 1993). Solum thickness was determined as the total thickness of the A and B horizons. The A horizon was identified by dark-coloured material, the B horizon by a uniform brown colour and the C horizon by the chalk-coloured parent material. Depth to calcium carbonate was determined by visible effervescence with 10% HCl (Soil Classification Working Group, 1998).

### 3.2. Digital terrain modelling

An irregular DEM of the study site based on 4211 points was constructed with a GPS technique (Parkinson and Spilker, 1996). The GPS receivers were single-frequency Trimble 4600LS Surveyors mounted on all-ter-

rain vehicles; data were collected cinematically. Vertical and horizontal accuracy of the DEM was 0.05 and 0.03 m, respectively.

The irregular DEM was converted into a regular one (Fig. 2) by the Delaunay triangulation and a piecewise smooth interpolation (Watson, 1992). The grid interval of the regular DEM was 15 m corresponding to typical sizes of microtopographic elements within the site. We calculated digital models of  $G$ ,  $A$ ,  $k_h$ ,  $k_v$ , mean curvature ( $H$ ), and accumulation curvature ( $K_a$ ) (Fig. 3(a)–(e)) by the method of Evans (1980), and applied the method of Martz and De Jong (1988) to calculate digital models of specific catchment area (CA), TI, and stream power index (SI) (Fig. 3(f)–(h)) using LANDLORD software (Florinsky et al., 1995). Each derived DTM has the grid interval of 15 m and consists of 2743 points.

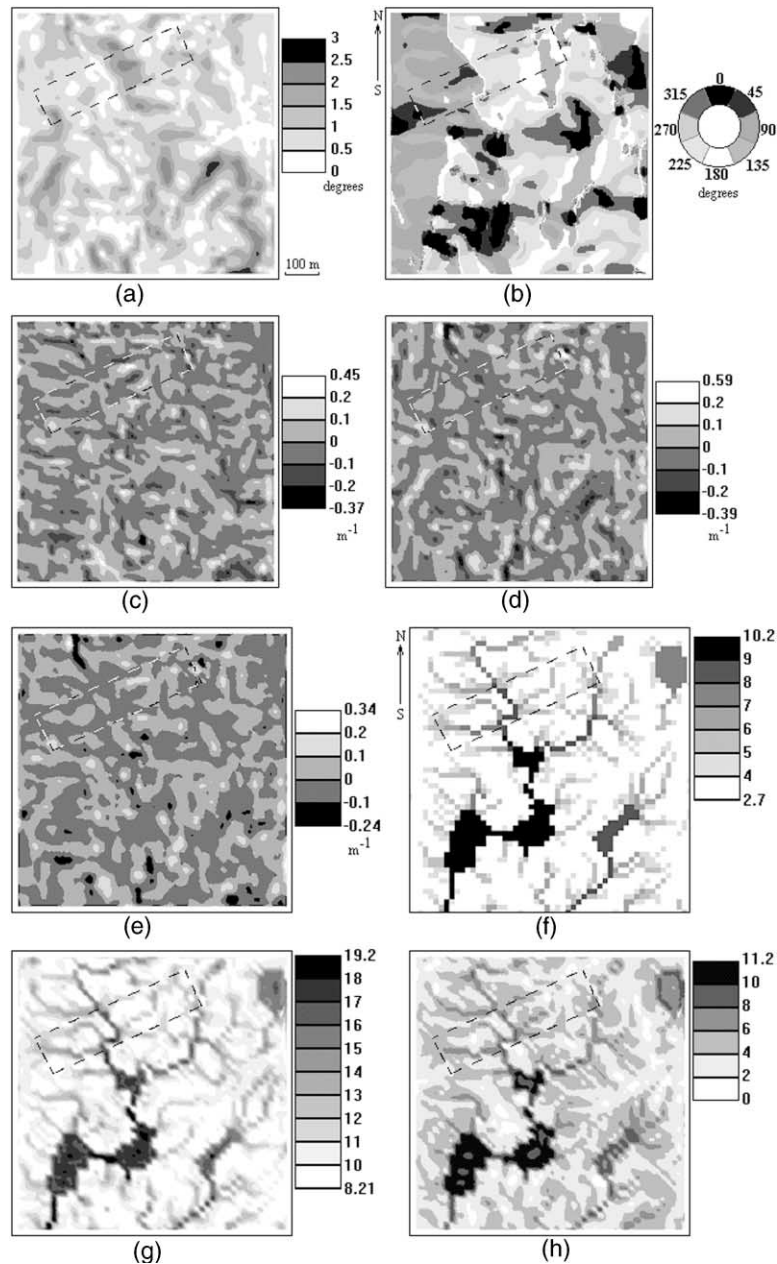


Fig. 3. The study site, topographic variables: (a) gradient, (b) aspect, (c) horizontal curvature, (d) vertical curvature, (e) mean curvature, (f) natural logarithm of specific catchment area, (g) topographic index, (h) stream power index. Dashed lines indicate the plot.

Then we used the Delaunay triangulation and a piecewise smooth interpolation of these DTMs to determine values of elevation ( $z$ ),  $G$ ,  $A$ ,  $k_h$ ,  $k_v$ ,  $H$ ,  $K_a$ ,  $CA$ ,  $TI$ , and  $SI$  at each of the 210 sampling points.

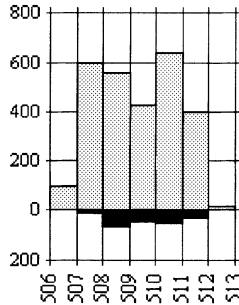
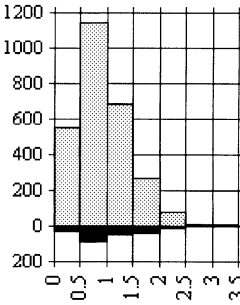
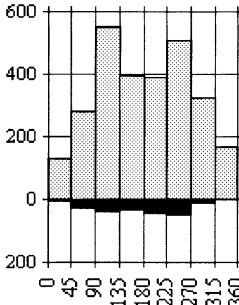
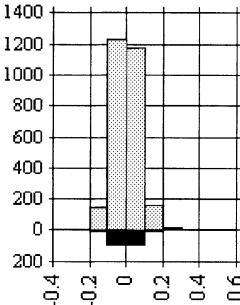
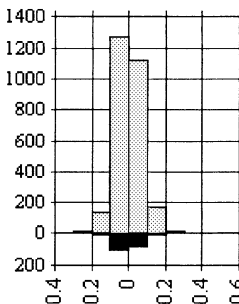
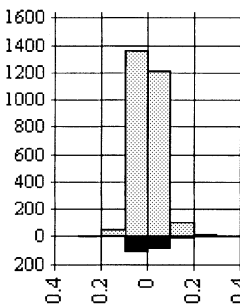
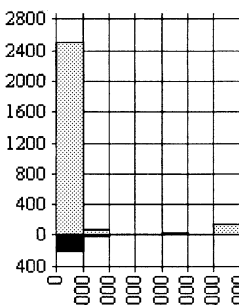
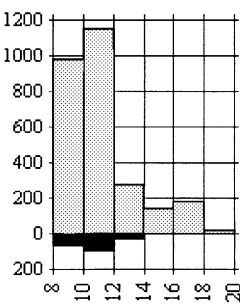
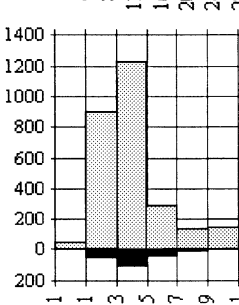
### 3.3. Statistical analysis

To estimate a topographic representativeness of the plot, we performed a comparative analysis of the statistical distribution of topographic variables within both the plot and the entire area of the site using a 210- and 2743-point samples, respectively (Table 3).

To evaluate relationships between soil properties and topographic attributes within the plot, we carried out multiple linear correlation analysis of gravimetric soil moisture and residual phosphorus estimated in different seasons and at different depths, solum thickness, depth to calcium carbonate, and organic carbon content with  $z$ ,  $G$ ,  $A$ ,  $k_h$ ,  $k_v$ ,  $H$ ,  $CA$ ,  $TI$ , and  $SI$  (Table 4).

To describe relationships between soil properties and topographic variables, the 'best' combinations of  $z$ ,  $G$ ,  $k_h$ ,  $k_v$ , and  $CA$  were chosen by stepwise linear regression (Aivazyan et al., 1985).  $H$ ,  $TI$  and  $SI$  were not included into the regression analysis since  $SI$  and  $TI$  are combi-

Table 3  
Statistical distribution of topographic variables within the study site and the plot

Diagrams	Study site	Plot	Diagrams	Study site	Plot
	<b>Elevation</b>			<b>Gradient</b>	
	506.43	507.7		0	0.04
	512.14	511.84		3.5	2.41
	509.3	509.68		0.97	1.03
	2.11	1.3		0.25	0.26
	1.45	1.14		0.5	0.51
	<b>Aspect</b>			<b>Horizontal curvature</b>	
	1.2	27.45		-0.37	-0.14
	359.9	313.91		0.46	0.23
	183	173.76		0	0.01
	7308.54	4646.29		0.01	0
	85.49	68.16		0.07	0.07
	<b>Vertical curvature</b>			<b>Mean curvature</b>	
	-0.39	-0.16		-0.24	-0.1
	0.6	0.22		0.35	0.19
	0	0		0	0
	0.01	0		0	0
	0.07	0.06		0.06	0.05
	<b>Specific catchment area</b>			<b>Topographic index</b>	
	15	15		8.22	8.56
	26,789	6524		19.27	17.47
	1708.92	291.11		11.16	10.92
	3,502,630	91,146		4.68	2.53
	5918.3	954.7		2.16	1.59
	<b>Stream power index</b>				
	-0.44	0.46			
	10.77	7.85			
	4.03	3.91			
	4.29	1.95			
	2.07	1.4			

(upper grey and lower black subgraphs describe distribution within the study site and the plot, correspondingly. Point number is along the y-axis. Counts are 2743 and 210 points for the entire study site and the plot, correspondingly. Each variable is described by minimum, maximum, average values, variance, and standard deviation)

Table 4  
Pairwise coefficients of linear correlation of soil properties with topographic variables

Soil property	Depth, m	Season	Sample size	$z$	$G$	$A$	$k_h$	$k_v$	$H$	CA	TI	SI
Soil moisture	0–0.3	05/97	209	–0.43*	–0.25*	ns	–0.26*	–0.45*	–0.41*	0.28*	0.40*	0.25*
		07/97	210	–0.42*	–0.29*	ns	–0.33*	–0.44*	–0.45*	0.35*	0.51*	0.33*
		08/97	210	–0.35*	–0.21*	ns	–0.17 <sup>+</sup>	–0.34*	–0.29*	0.24*	0.28*	ns
		05/98	210	–0.43*	–0.22*	ns	–0.30*	–0.48*	–0.45*	0.30*	0.47*	0.37*
		07/98	209	–0.31*	–0.30*	–0.25*	–0.17 <sup>+</sup>	–0.25*	–0.25*	0.21*	0.32*	ns
	0.3–0.6	08/98	210	–0.39*	–0.27*	ns	–0.24*	–0.42*	–0.38*	0.26*	0.38*	0.21*
		05/97	209	–0.26*	ns	0.19 <sup>+</sup>	ns	–0.21*	–0.17 <sup>+</sup>	ns	ns	ns
		07/97	209	–0.26*	–0.19 <sup>+</sup>	0.15 <sup>+</sup>	ns	–0.28*	–0.24*	0.20*	0.23*	ns
		08/97	209	–0.19*	–0.22*	ns	–0.18 <sup>+</sup>	–0.27*	–0.26*	0.27*	0.27*	ns
		05/98	210	–0.40*	ns	0.25*	–0.23*	–0.35*	–0.33*	0.32*	0.35*	0.32*
	0.6–0.9	07/98	209	–0.27*	–0.17 <sup>+</sup>	–0.17 <sup>+</sup>	ns	–0.15 <sup>+</sup>	ns	0.22*	0.21 <sup>+</sup>	ns
		08/98	210	–0.26*	ns	0.13 <sup>+</sup>	ns	–0.20 <sup>+</sup>	ns	ns	ns	ns
		05/97	209	–0.29*	ns	0.16 <sup>+</sup>	ns	–0.23*	–0.20*	0.18 <sup>+</sup>	0.18 <sup>+</sup>	ns
		07/97	206	–0.19 <sup>+</sup>	ns	ns	ns	ns	ns	0.16 <sup>+</sup>	ns	ns
		05/98	210	–0.35*	ns	0.23*	ns	–0.26*	–0.21*	0.21*	0.17 <sup>+</sup>	0.18 <sup>+</sup>
	0.9–1.2	07/98	209	–0.28*	–0.16 <sup>+</sup>	–0.15 <sup>+</sup>	ns	ns	ns	0.24*	ns	ns
		08/98	210	–0.26*	ns	ns	ns	–0.19 <sup>+</sup>	ns	ns	ns	ns
		05/97	209	–0.22*	ns	0.15 <sup>+</sup>	ns	–0.19*	ns	0.16 <sup>+</sup>	ns	ns
		07/97	200	–0.33*	ns	ns	ns	–0.22*	–0.16 <sup>+</sup>	0.24*	0.22*	ns
		05/98	210	–0.26*	ns	0.20*	–0.14 <sup>+</sup>	–0.24*	–0.22*	0.20 <sup>+</sup>	0.21*	ns
Residual phosphorus	0–0.3	07/98	205	–0.40*	ns	ns	ns	–0.16 <sup>+</sup>	–0.15 <sup>+</sup>	0.18 <sup>+</sup>	0.16 <sup>+</sup>	ns
		08/98	210	–0.16 <sup>+</sup>	ns	ns	ns	ns	ns	0.15 <sup>+</sup>	0.15 <sup>+</sup>	ns
	0.3–0.6	05/97	210	–0.22*	–0.14 <sup>+</sup>	ns	–0.18 <sup>+</sup>	–0.32*	–0.29*	0.23*	0.31*	0.22*
		05/98	210	–0.30*	–0.22*	ns	–0.24*	–0.35*	–0.35*	0.41*	0.42*	0.27*
	0.6–0.9	05/97	210	–0.30*	–0.23*	ns	–0.17 <sup>+</sup>	–0.34*	–0.29*	0.38*	0.42*	0.26*
		05/98	210	–0.19*	–0.25*	ns	ns	–0.24*	–0.19*	0.28*	0.33*	0.14 <sup>+</sup>
	0.9–1.2	05/97	210	Ns	–0.16 <sup>+</sup>	ns	–0.14 <sup>+</sup>	–0.24*	–0.22*	ns	0.21*	ns
		05/98	210	Ns	–0.24*	ns	ns	–0.24*	–0.21*	0.22*	0.24*	ns
	05/97	210	Ns	ns	ns	ns	ns	ns	ns	ns	ns	
	05/98	210	Ns	–0.23*	ns	ns	ns	ns	ns	0.15 <sup>+</sup>	0.18 <sup>+</sup>	ns
Solum thickness			210	–0.22*	–0.18 <sup>+</sup>	ns	–0.25*	–0.39*	–0.37*	0.26*	0.35*	0.26*
Depth to calcium carbonate			210	–0.16 <sup>+</sup>	–0.18 <sup>+</sup>	ns	–0.24*	–0.42*	–0.38*	0.24*	0.33*	0.24*
Organic carbon content			209	–0.42*	–0.31*	–0.24*	–0.34*	–0.45*	–0.46*	0.26*	0.48*	0.32*

(\*significance level is 0.00; <sup>+</sup>significance level is between 0.01 and 0.05; ns — statistically non-significant correlations)



nations of  $G$  and  $CA$ , while  $H$  is a combination of  $k_h$  and  $k_v$  (Table 1).  $A$  was omitted from the linear regression, as it is a circular variable (Section 4.1).

Several regression equations with  $R^2 \geq 0.25$  (Table 5) were then used to predict the spatial distribution of soil properties within the entire area of the site. The regression-based predictive maps (Fig. 4) were obtained using digital models of topographic attributes inserted into the corresponding regression equations as independent variables (Table 5). Predictive values of soil moisture, residual phosphorus and organic carbon content were calculated for 2743 points of DTM square-spaced grid.

The statistical analysis was carried out by STATGRAPHICS Plus 3.0 software (Statistical Graphics Corp.). Predictive maps (Fig. 4) were produced by LANDLORD software (Florinsky et al., 1995).

### 3.4. Concept of accumulation, transit and dissipation zones

The concept of topographically expressed accumulation, transit and dissipation zones is based on the following assumptions. Gravity-driven overland and intra-soil transport can be interpreted in terms of divergence or convergence, and deceleration or acceleration of flows (Shary, 1995). Flow tends to accelerate when  $k_v > 0$ , and to decelerate when  $k_v < 0$  (Table 1) (Speight, 1974; Shary, 1991). Flow diverges when  $k_h > 0$ , and converges when  $k_h < 0$  (Table 1) (Kirkby and Chorley, 1967; Shary, 1991). Flow convergence and deceleration result in accumulation of substances in soils. At different scales, the spatial distribution of accumulated substances can depend on the distribution of the following landforms (Shary et al., 1991; Florinsky, 2000): (a) those marked both by convergence and deceleration of flow, that is, both by  $k_h < 0$  and by  $k_v < 0$  (accumulation zones); (b) those offering both divergence and acceleration of flow, that is, both  $k_h > 0$  and  $k_v > 0$  (dissipation zones); and (c) those that are free of a concurrent action of flow convergence and deceleration as well as divergence and acceleration, that is, values of  $k_h$  and  $k_v$  have different signs or are zero (transit zones).

Recognition of landsurface zones can be done by registration of  $k_h$  and  $k_v$  maps (Koshkarev, 1982; Lanyon and Hall, 1983), or by combination of  $K_a$  and  $H$  data (Shary, 1995) (Table 1). Negative values of  $K_a$  correspond to transit zones, and positive values of  $K_a$  correspond to both accumulation and dissipation zones. Accumulation and dissipation zones can be distinguished using  $H$ . Positive values of  $K_a$  with negative values of  $H$  correspond to accumulation zones, whereas positive values of  $K_a$  with positive values of  $H$  correspond to dissipation zones. A map of accumulation, transit and

dissipation zones (Fig. 5) was obtained using  $H$  and  $K_a$  data by LANDLORD software (Florinsky et al., 1995).

Prediction of soil property distributions with the concept of landsurface zones included the following steps: First, we used the map of these zones (Fig. 5) to locate the sampling points. Of the 210 points, 51, 84 and 75 are situated in accumulation, transit and dissipation zones, respectively. Second, we estimated means and standard deviations of soil properties for the landforms within the plot (Table 6). Third, we developed diagrams of the distributions of the means over the landforms (Fig. 6). Fourth, we obtained ratios of means, that is, ratios between the mean for either the transit or accumulation zones to the mean of the dissipation zone for soil properties marked by strong regular distributions over landforms (Table 6): soil moisture at 0–0.3 m depth, residual phosphorus at 0–0.3 m depth, solum thickness, depth to calcium carbonate, and organic carbon content. We selected means at dissipation zones because water supplied to a sizeable area of these zones (e.g. tops, water divides and crests) is from the atmosphere only, so there are no substances received by these zones from neighbouring areas. Finally, we computed time-average ratios of means for soil moisture and residual phosphorus content at the 0–0.3 m depth (Table 6). To estimate the absolute mean of a soil property at other terrains marked by similar natural conditions, one has to (a) measure this property in some dissipation zones, (b) calculate a mean of these measurements in the dissipation zones, and (c) multiply this value by all other ratios of means.

To validate this approach and to compare it with regression-based prediction, we used data on solum thickness estimated within the entire area of the site. Intact 0.04 m diameter soil cores in polyethylene sleeves have been obtained by a truck-mounted hydraulic coring device at 37 random points (Fig. 1) (Fitzmaurice et al., 1999). These 37 points are independent of the 210 points used in statistical analysis and in estimation of ratios of means (Fig. 1). There were no independent data on other soil attributes at the 37 points. First, we used the map of landsurface zones (Fig. 5) to locate these points. Of the 37 points, 13, 13 and 11 were situated in accumulation, transit and dissipation zones, respectively. Second, using a 5-point random sample from the 11 points situated in dissipation zones, we estimated the absolute mean solum thickness at dissipation zones of the study site to be 0.32 m. A 5-point sample was used as we assume that the prediction of soil properties by the concept of landsurface zones can allow one to minimise number of field sampling and measurements. Third, using ratios of means for the solum thickness (Table 6), we predicted absolute mean solum thickness at accumulation and transit zones to be 0.67 and 0.45 m, respectively. Fourth, we estimated values of the solum thickness at each of the 37 points by the regression equation and

Table 5  
Parameters of regression equations describing dependencies of some soil properties on topographic variables, and analysis of variance for regression equations

Dependent variables	Soil moisture				Residual phosphorus		Organic carbon content	Solum thickness
	0–0.3 m, 05/97	0–0.3 m, 07/97	0–0.3 m, 05/98	0–0.3 m, 08/98	0–0.3 m, 05/98	0.3–0.6 m, 05/97		
Constant	551.02	368.22	431.77	406.99	444.9	165.17	81.23	41.34
Independent variables								
$z$	–1.03	–0.68	–0.80	–0.76	–0.84	–0.32	–0.15	
$G$	–2.06	–1.58	–1.45	–1.76	–2.87	–0.99	–0.37	–4.86
$k_h$		–4.55	–3.58				–1.06	
$k_v$	–19.78	–12.49	–18.87	–14.37	–38.96	–10.97	–2.48	–113.84
CA		0.0004	0.0003		0.003	0.0007		0.003
Model								
Sum of squares	1021.78	694.47	925.32	584.74	4858.9	403.70	26.62	13736.5
Df	3	5	5	3	4	4	4	3
Mean square	340.59	138.89	185.06	194.91	1214.72	100.92	6.66	4578.84
$F$ -ratio	33.03	23.93	21.40	30.13	18.57	16.74	30.18	17.32
$p$ -Value	0.00	0.00	0.00	0.00	0.00	0.00	0.00	0.00
Residual								
Sum of squares	2113.88	1184.2	1764.4	1332.73	13406.4	1235.62	44.99	54465.1
Df	205	204	204	206	205	205	204	206
Mean square	10.31	5.81	8.65	6.47	65.40	6.03	0.22	264.39
$R^2$	0.33	0.37	0.34	0.31	0.27	0.25	0.37	0.20
Standard error	3.21	2.40	2.94	2.54	8.09	2.46	0.47	16.26
Mean error	2.49	1.81	2.20	2.00	6.22	1.61	0.36	11.92
Durbin-Watson	1.87	1.60	1.64	1.70	1.89	2.06	1.75	2.30

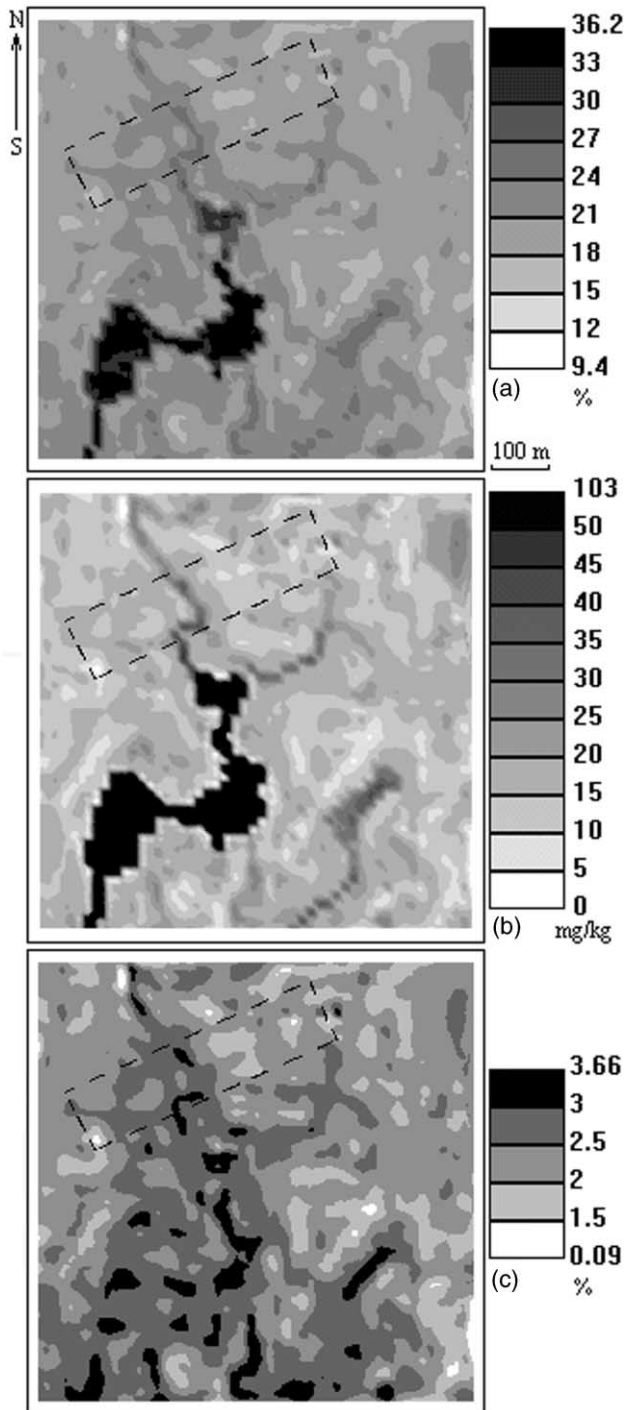


Fig. 4. Regression-based prediction of soil properties: (a) soil moisture content, the 0–0.3 m depth, July 1997, (b) residual phosphorus content, the 0–0.3 m depth, May 1998, (c) organic carbon content of the A horizon. Dashed lines indicate the plot.

corresponding DTMs (Table 5). Finally, we compared actual values of the solum thickness with its values predicted both by the concept of landsurface zones and by the regression.

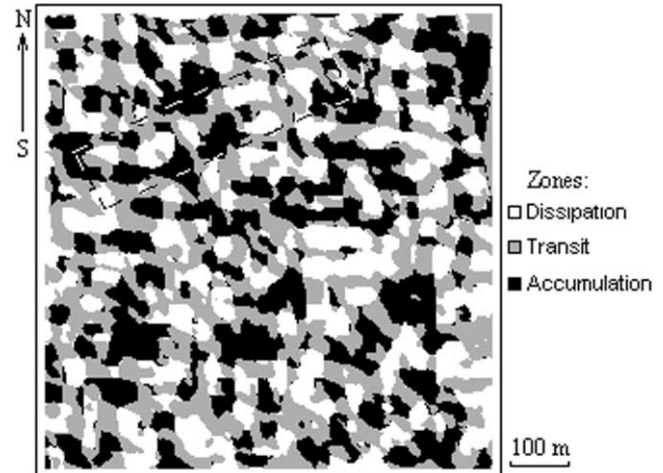


Fig. 5. The study site, accumulation, transit and dissipation zones. Dashed lines indicate the plot.

## 4. Results and discussion

### 4.1. Correlation and regression analyses

The comparative analysis of the statistical distribution of topographic variables within the plot and the entire area of the site demonstrated that the plot is generally representative of the site for the topographic attributes (Table 3). Exceptions are the distributions of CA, TI and SI (Table 3). This was expected since they are non-local topographic variables and accumulate their values downslope. It is hard to choose a plot taking into complete account statistical distributions of these topographic variables.

The correlation analysis (Table 4) showed that soil moisture at the 0–0.3 m depth was dependent on all topographic variables except  $A$ . Generally, this was obvious and supported by the results of previous investigations and physical interpretations of topographic variables (Table 1). For example, as  $G$  increases, velocity of water flow and slope area increase, so the rainfall received per unit area and its infiltration decrease, the runoff and evaporation area increase, and hence soil moisture decreases (Zakharov, 1940). This leads to negative correlations between soil moisture and  $G$  (Table 4).

$k_h$  and  $k_v$  are the determining local factors of the dynamics of overland and intrasoil water (Table 1). Soil moisture and lateral intrasoil flow increase if  $k_h < 0$  or  $k_v < 0$ , and decrease if  $k_h > 0$  or  $k_v > 0$  (Kirkby and Chorley, 1967; Anderson and Burt, 1978; Burt and Butcher, 1985). This leads to negative correlations of soil moisture with  $k_h$  and  $k_v$  (Table 4). Since soil moisture had higher correlations with  $k_v$  than with  $k_h$ , relative deceleration is the main mechanism controlling flow accumulation in the site. Negative correlations of soil moisture with  $H$  (Table 4) resulted from the fact that  $H$  presents

Table 6

Means, standard deviations, and ratios of means for soil properties at dissipation, transit and accumulation zones

Soil property	Dissipation zone			Transit zone			Accumulation zone		
	Mean	Standard deviation	Ratio of means	Mean	Standard deviation	Ratio of means	Mean	Standard deviation	Ratio of means
Soil moisture, 0–0.3 m, 05/97	20.4	3.3	1	22.4	3.3	1.10	25.1	3.9	1.23
Soil moisture, 0–0.3 m, 05/98	18.3	2.6	1	20.5	3.0	1.12	23.1	3.7	1.26
Soil moisture, 0–0.3 m, 07/97	19.1	2.2	1	20.0	3.1	1.05	22.0	3.1	1.15
Soil moisture, 0–0.3 m, 07/98	25.5	3.5	1	26.7	3.2	1.05	28.4	4.3	1.11
Soil moisture, 0–0.3 m, 08/97	14.8	2.8	1	15.8	3.0	1.07	16.4	3.5	1.11
Soil moisture, 0–0.3 m, 08/98	19.2	2.6	1	20.5	2.8	1.07	22.3	3.2	1.16
Average soil moisture, 0–0.3 m			1			1.08			1.17
Residual phosphorus, 0–0.3 m, 05/97	11.5	6.7	1	15.2	8.2	1.32	17.9	9.9	1.56
Residual phosphorus, 0–0.3 m, 05/98	12.1	7.2	1	15.7	8.6	1.30	22.1	10.2	1.83
Average residual phosphorus, 0–0.3 m			1			1.31			1.70
Solum thickness	0.26	0.08	1	0.37	0.15	1.42	0.54	0.21	2.08
Depth to calcium carbonate	0.23	0.10	1	0.35	0.18	1.52	0.55	0.25	2.39
Organic carbon content, A horizon	2.0	0.4	1	2.3	0.5	1.15	2.8	0.6	1.40

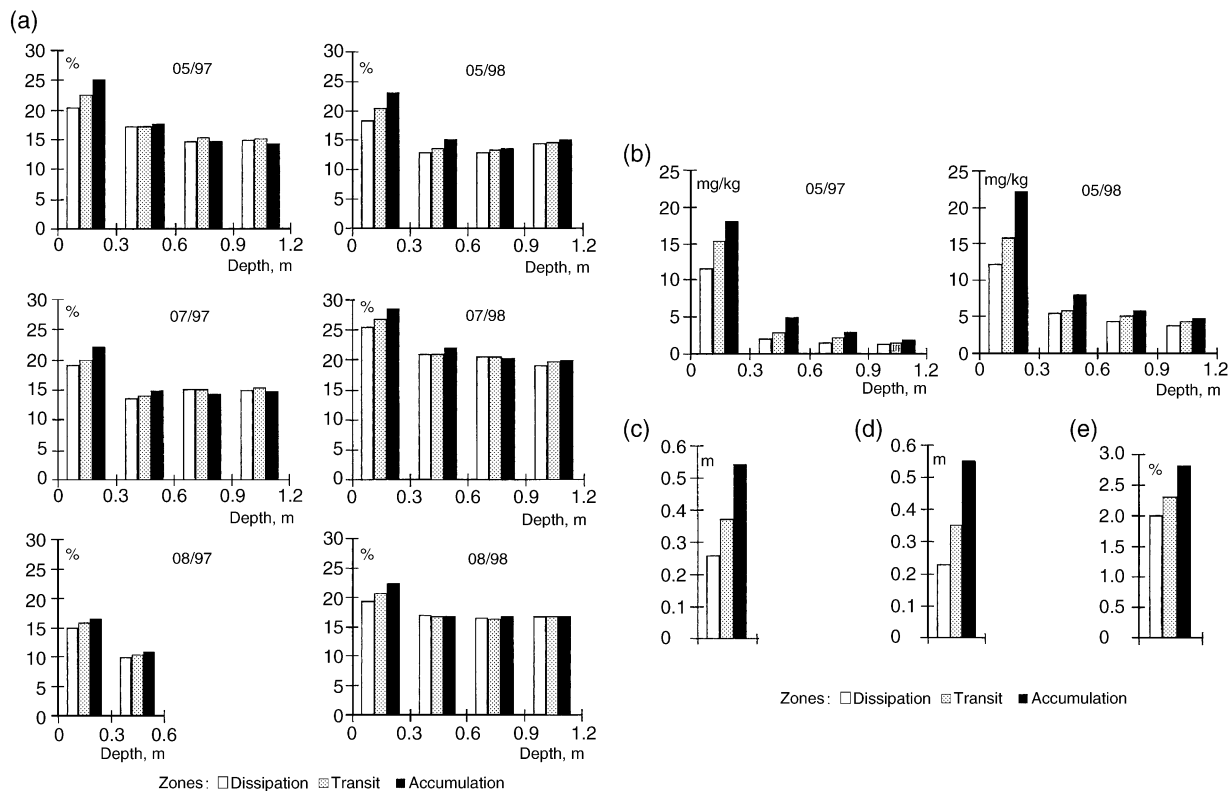


Fig. 6. Distribution of means of soil properties over accumulation, transit and dissipation zones: (a) gravimetric soil moisture content, (b) residual phosphorus content, (c) solum thickness, (d) depth to calcium carbonate, (e) organic carbon content of the A horizon.

flow convergence and deceleration with equal weights (Florinsky and Kuryakova, 2000) (Table 1).

Positive correlations of soil moisture with CA (Table 4) stem from an increase of moisture per unit area along a slope from top to bottom, because of additional water contributed from upslope units (Table 1) (Zakharov, 1940). Thus, as CA increases, soil moisture also increases. CA can play a more dominant role in the con-

trol of soil water redistribution than landsurface curvatures, since CA takes into account the location of a point in the landscape (Speight, 1980). Note that the dependence of soil moisture on  $z$  (Tables 4 and 5) was also the result of the influence of CA on soil moisture. This is because  $z$  is not responsible in itself for physical mechanisms of gravity-driven moisture movement. However,  $z$  is taken into account in CA calculation in a

hidden form (Speight, 1968; Martz and De Jong, 1988). A dependence of this sort can also be observed for vegetation cover (Florinsky and Kuryakova, 1996).

TI (Table 1) can provide further improvement in description of the spatial distribution of the soil moisture (Burt and Butcher, 1985). This is because TI takes into account both a local slope geometry and location of a point in the landscape, combining data on  $G$  and  $CA$  (Gessler et al., 1995). As  $CA$  increases and  $G$  decreases, TI and soil moisture increase. This resulted in higher absolute correlations of soil moisture with TI than with  $CA$  and  $G$  (Table 4).

SI (Table 1) can be used to describe potential flow erosion and related landscape processes (Moore et al., 1993). Like TI, SI combines with  $G$  and  $CA$ . As  $CA$  and  $G$  increase, the amount of water contributed by upslope areas and the velocity of water flow increase, hence SI and erosion risk increase. This resulted in positive correlations between SI and some soil properties (Table 4).

The soil water balance is influenced by  $A$ , since, in association with  $G$ ,  $A$  impacts insolation and evapotranspiration (Romanova, 1977). In the northern hemisphere, moisture content tends to be highest on north slopes, intermediate on west and east slopes, and least on south slopes (Ponagaibo, 1915; Zakharov, 1940). However, there were scarcely any significant correlations between soil moisture and  $A$  within the plot (Table 4). This may be because insolation and evapotranspiration do not effect essentially the spatial variability of soil moisture in relatively flat landscapes of this climatic zone. Also, the lack of significant correlations with  $A$  may be connected with a circular character of  $A$  (Hodgson and Gaile, 1996; King et al., 1999). It is more correct to apply methods of circular statistics in this case (Mardia, 1972; Batschelet, 1981). However, these approaches were outside the scope of the study.

For the 0–0.3 and 0.3–0.6 m depths, correlation coefficients suggested that topography influences the spatial distribution of phosphorus (Table 4) through the control of soil moisture regime (Kovda, 1973; Moore et al., 1993). Residual phosphorus was most strongly dependent on TI,  $CA$ ,  $k_v$ , and  $H$  (Table 4).

The correlations describing relationships of the soil moisture and residual phosphorus with topography differed among seasons (Table 4). This is an evidence of a temporal variability in soil–topography relationships. Absolute values of the correlation coefficients of the soil moisture and residual phosphorus with relief attributes decreased and at times were non-significant with increasing soil depth (Table 4). This demonstrated a decrease of the topographic influence on soil properties with depth.

We found relatively high correlation coefficients for solum thickness and depth to calcium carbonate with  $k_v$ ,  $H$ , and TI (Table 4). This confirmed well-known facts about topographic influence on the thickness of soil horizons (Zakharov, 1940; Aandahl, 1948; Pennock et al.,

1987; Moore et al., 1993; Bell et al., 1994; Odeh et al., 1994; Gessler et al., 1995) and depth to calcium carbonate (Ponagaibo, 1915; Walker et al., 1968; Bell et al., 1994; Florinsky and Arlashina, 1998) in various natural conditions. This is because the solum thickness and depth to calcium carbonate are controlled by overland and intrasoil water dynamics depending on relief. The same trend was apparent for correlations of organic carbon content with topographic characteristics (Table 4). This resulted from a dependence of organic carbon on the spatial differentiation of organic matter accumulation and moistening according to landsurface morphology (Kovda, 1973; Moore et al., 1993; Arrouays et al., 1998).

All topographic variables are derived from  $z$  (Table 1). Also, SI and TI are functions of  $G$  and  $CA$ , and  $H$  is a function of  $k_h$  and  $k_v$  (Table 1). These relations may influence correlations between topographic and soil attributes. From the statistical standpoint, one should perform an analysis of partial correlations between soil and topographic attributes to neutralise this effect. A partial correlation coefficient measures a relationship between two variables and controls for possible effects of the other variables (Aivazyán et al., 1985). However, from the physical viewpoint, this statistics is meaningless in the case. Indeed, we study dependencies of soil properties on landscape processes of gravity-driven overland and intrasoil transport rather than on mathematical functions of  $z$ ,  $k_h$ ,  $k_v$ , etc. Topographic control of soil properties is provided not by mathematical functions but by slope shapes determining velocity, direction, convergence and acceleration of flows (mathematically described by  $G$ ,  $A$ ,  $k_h$  and  $k_v$ , respectively) as well as by relative position in the landscape (described by  $CA$ ). Each topographic variable is a measure of a *specific* gravity-driven process or mechanism. For example, one may analyse correlations between a soil property and SI, a function of  $G$  and  $CA$  (Table 1), to study the dependence of the soil property on erosion. There are no reasons to compensate for the effects of  $G$  and  $CA$  in this case, since SI is just their combination providing description of erosion processes. At the same time,  $z$  is not responsible in itself for any gravity-driven mechanism and process. So, from the physical viewpoint, it is unclear what kind of effect of  $z$  can be neutralised by an analysis of partial correlations.

Most of the regression equations obtained had  $R^2 < 0.25$ , we did not include them in Table 5 except an equation for the solum thickness. We obtained four regression equations with  $R^2 \geq 0.25$  for soil moisture at 0–0.3 m depth in different seasons (Table 5). There were different coefficients and sets of independent variables in the equations for different seasons. This is a further evidence of the temporal variability in soil–topography relationships.  $R^2$  values were not greater than 0.37, so up to 37% of soil moisture variability for the 0–0.3 m depth was explained by topographic attributes. Also, we

obtained regression equations explaining 27 and 25% of the variability of phosphorus distribution for the 0–0.3 and 0.3–0.6 m depths, respectively, and 37% of the variability of organic carbon content (Table 5).

The relatively low  $R^2$  values obtained (Table 5) were expected because we worked in the low relief landscape and considered only the topographic prerequisites for spatial distribution of soil properties. Other factors (i.e. bulk density and soil texture, Table 2) were ignored. Sometimes, higher values of  $R^2$  may be obtained by increasing DTM resolution (Moore et al., 1993). Generally,  $R^2$  values for topographic variables are in the range of 0.39–0.82 for different soil properties examined in other landscapes with a more distinct topography (Pennock et al., 1987; Moore et al., 1993; Bell et al., 1994; Odeh et al., 1994; Gessler et al., 1995; Florinsky and Arlashina, 1998; Florinsky and Kuryakova, 2000).

Predictive maps of soil properties (Fig. 4) show that regression-based prediction may identify the spatial distribution of soil attributes. However, different regression equations are obtained for different seasons for temporally dynamic soil variables. This limits the widespread utility of the approach.

#### 4.2. Concept of accumulation, transit and dissipation zones

The diagrams of soil moisture distribution over landscape zones demonstrated a strong trend for the 0–0.3 m depth. Accumulation, transit, and dissipation zones are marked by maximum, medium, and minimum soil moisture, respectively (Fig. 6(a)). This regularity was less defined and disappeared with depth. The similar trend was observed for the residual phosphorus (Fig. 6(b)), solum thickness (Fig. 6(c)), depth to calcium carbonate (Fig. 6(d)), and organic carbon content (Fig. 6(e)). These were expected results as saturation zones, maximum thickness of the A horizon and depth to calcium carbonate correlate with landforms marked by negative values of both  $k_h$  and  $k_v$  due to increased accumulation of water there (Pennock et al., 1987; Feranec et al., 1991).

Accumulation zones showed the largest standard deviations for all soil properties, and dissipation zones showed the lowest ones (Table 6). This is because a sizeable area of dissipation zones (e.g. water divides) receives water from the atmosphere only. So, they receive an approximately equal amount of water per unit area, and have much the same water regime throughout the landscape. At the same time, different upslope areas contribute various amounts of water to the various accumulation zones in addition to atmosphere water. This results in dissimilar moisture regimes in different depressions. Indeed,  $\ln(CA)$  ranged from 2 to 4 in dissipation zones, but from 2 to 11 in accumulation zones (Fig. 7). To decrease standard deviations of soil proper-

ties in accumulation zones and improve prediction, accumulation zones may be parted into groups marked by different ranges of  $\ln(CA)$ . Means and ratios of means for soil properties may be evaluated within these groups (this procedure was not done in the study).

#### 4.3. Validation

A comparison of actual solum thickness and its values predicted by the concept of landscape zones demonstrated that crests were characterised by the highest accuracy of prediction, whereas depressions were the least accurate (Fig. 8). Absolute mean prediction errors for dissipation, transit and accumulation zones were 0.03, 0.04 and 0.11 m, respectively. In part, this resulted from the greater deviations of solum thickness in accumulation zones, and the smaller deviations in dissipation zones (Fig. 8). The total absolute mean error of the prediction was 0.06 m. However, mean absolute errors ranged from 0.00 to 0.03 m at 16 points (9, 4 and 3 points in dissipation, transit and accumulation zones, respectively) (Fig. 8). This was near the accuracy of the field estimation of solum thickness (Soil Classification Working Group, 1998). Absolute mean errors were 0.00 m at four points in transit zones (Fig. 8). Two points were marked by an absolute mean error of 0.13 m and two points by 0.33 m in accumulation zones (Fig. 8). Obviously, a change of the number and specific values of samples for estimation of the absolute mean solum thickness in dissipation zones (Section 3.4) can influence the prediction. Nevertheless, the prediction by landscape zoning explains 97% of the variability of the solum thickness.

A comparison of actual solum thickness and its values predicted by the linear regression showed that absolute mean prediction errors for dissipation, transit and accumulation zones were 0.06, 0.10 and 0.34 m, respectively (Fig. 8). The total absolute mean error of the prediction was 0.17 m. Mean absolute errors ranged from 0.00 to 0.03 m at six points only (Fig. 8). Seventeen points were marked by absolute mean errors of 0.13 m and more including 0.47, 0.61 and 0.71 m (Fig. 8). The linear regression equation of the solum thickness explains only 20% of the spatial variability of the solum thickness (Table 5).

The validation results showed that the application of the concept of landscape zones to predict the spatial distribution of the solum thickness was more successful than the prediction based on the linear regression. However, additional studies are required to validate the accuracy of the concept of landscape zones for the prediction of other soil properties.

#### 4.4. General discussion

The temporal variability in relationships between soil and topographic attributes exists because soil properties

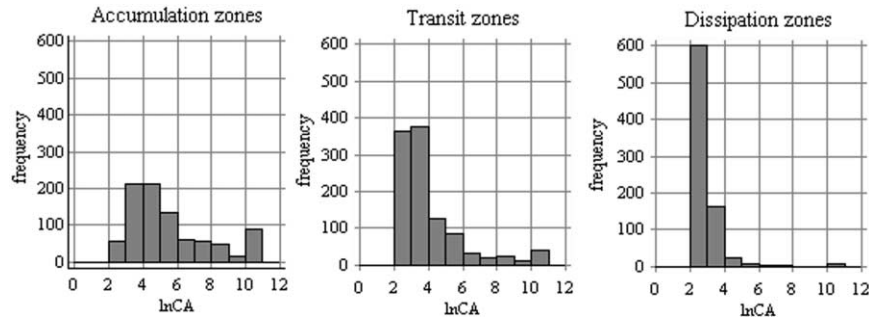


Fig. 7. Distribution of values of the natural logarithm of specific catchment area over accumulation, transit and dissipation zones.

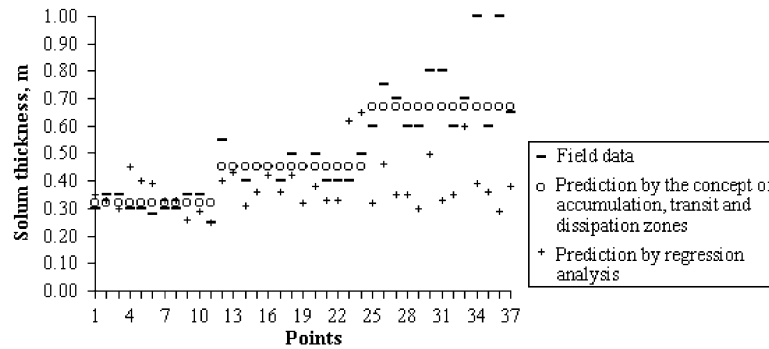


Fig. 8. Solum thickness: actual and predicted values obtained with the concept of accumulation, transit and dissipation zones and regression analysis.

are the result of an integration of various processes with different temporal variabilities (Dokuchaev, 1892; Jenny, 1961; Huggett, 1975; Gerrard, 1981; Stepanov et al., 1991). As erosion and deposition change the landscape relatively slowly, so relief attributes can be seen as temporally stable determinants of soil development. Other factors, such as plant characteristics, have high temporal variability. This leads to temporal variability in a spatially distributed soil response, which can be observed as temporal variability in relationships between soil and topographic properties. The rate of this temporal variability may be connected with a dynamic rate of a soil property. For example, relationships between topography and relatively static soil attributes may be marked by a low temporal variability.

The strong temporal variability in soil–topography relationships was easily observable when we analysed them at each point in the landscape (Tables 4 and 5). Once we simplified the task and analysed the distribution of ratios of means for soil properties over landforms, temporal variability became less, at least for soil moisture (Table 6). For example, means of soil moisture in August 1997 and 1998 were 15.8 and 20.5%, respectively, and corresponding ratios of means were 1.07 (Table 6). This is because this simplification is a generalisation leading to data smoothing. We suppose that a simplification of this sort is a reasonable method for practical modelling of soil properties, since there is no

way to predict the overall variability of soil properties, as it is impossible to model the actual temporal and spatial variability in all pedogenetic factors.

The temporal variability in relationships between soil and topographic attributes may be in part a function of sampling variability. Minor changes could occur in samples as it is difficult to sample identical locations at different times.

The variability in relations between soil and topography with depth may stem from the spatial variability in the characteristic decline of hydraulic conductivity with depth (Table 2). If this decline was the same at all points in the landscape (as in TOPMODEL — Beven and Kirkby, 1979; Beven et al., 1995), we would have observed equal correlations between soil and topographic attributes for all depths examined. The spatial variability of the decline in hydraulic conductivity with depth can be associated with spatial variability of pedogenetic processes, the existence of relict soil patterns, and random inclusions of sand or silt lenses in glacial till. The strongest dependence of soil properties on topography occurred at the 0–0.3 m depth within the study site. We suppose that in different landscapes, one may observe different depth of ‘effective soil layers’, wherein relations of soil to topography are significant.

Temporal and depth variability in relations between soil and topography should be considered along with regional and scale variability in the topographic control

of soil attributes. Regional variability refers to distinctions in topographic control of soil properties under different natural conditions (Ponagaibo, 1915; Beven et al., 1995). Scale variability refers to the change in the character of soil-relief relations under changes in biogeocoenosis hierarchy and study scale (Florinsky and Kuryakova, 2000).

## 5. Conclusions

1. The dependence of soil properties on topography is obvious and is supported by correlations for the upper soil layer. However, the topographic control of soil moisture and residual phosphorus decreases with depth. The variability in relationships between some soil and topographic characteristics with depth may stem from spatial variability in the rate of decline of hydraulic conductivity with depth.
2. There is temporal variability in relationships between some soil and topographic attributes. Different correlation coefficients and regression equations describe the topographic control of soil moisture and residual phosphorus in different seasons. This is because soil properties are the result of interactions of various pedogenetic factors marked by different temporal variability. The temporal variability in the 'soil-topography' system imposes limits on regression-based soil predictions.
3. The prediction of soil property distribution with the concept of accumulation, transit and dissipation zones can be more successful and appropriate than the prediction based on linear regression.
4. In soil studies with digital terrain modelling, there is a need to take into account four types of variability in relations between soil and relief: regional, temporal, depth, and scale.

## Acknowledgements

The work was supported by the NSERC programs for Visiting Fellowships in Canadian Government Laboratories and the NSERC program for Postgraduate Scholarships. We are grateful to R. Bell for the use of his farm as well as anonymous referees for fruitful criticism.

## References

Aandahl, A.R., 1948. The characterization of slope positions and their influence on the total nitrogen content of a few virgin soils of western Iowa. *Soil Science Society of America Proceedings* 13, 449–454.

Aivazyan, S.A., Yenyukov, I.S., Meshalkin, L.D., 1985. *Applied Statistics: Study of Relationships*. Finansy i Statistika, Moscow (in Russian, with English contents).

Anderson, M.G., Burt, T.P., 1978. The role of topography in controlling throughflow generation. *Earth Surface Processes* 3 (4), 331–344.

Arrouays, D., Daroussin, J., Kicin, J.L., Hassika, P., 1998. Improving topsoil carbon storage prediction using a digital elevation model in temperate forest soils of France. *Soil Science* 163 (2), 103–108.

Batschelet, E., 1981. *Circular Statistics in Biology*. Academic Press, London.

Bell, J.C., Thompson, J.A., Butler, C.A., McSweeney, K., 1994. Modelling soil genesis from a landscape perspective. In: Etchevers, B.J.D. (Ed.), *Transactions of the 15th World Congress of Soil Science*, 6a. ISSS. Acapulco, Mexico (July 1994).

Beven, K.J., Kirkby, M.J., 1979. A physically-based variable contributing area model of basin hydrology. *Hydrological Science Bulletin* 24 (1), 43–69.

Beven, K.J., Lamb, R., Quinn, P., Romanowicz, R., Freer, J., 1995. topmodel. In: Singh, V.P. (Ed.), *Computer Models of Watershed Hydrology*. Water Resources Publications, Colorado.

Burrough, P.A., 1986. *Principles of Geographical Information Systems for Land Resources Assessment*. Clarendon Press, Oxford.

Burrough, P.A., 1993. Soil variability: a late 20th century view. *Soils and Fertilizers* 56 (5), 529–562.

Burt, T.P., Butcher, D.P., 1985. Topographic controls of soil moisture distribution. *Journal of Soil Science* 36 (3), 469–486.

Carter, M.R. (Ed.), 1993. *Soil Sampling and Methods of Analysis*. Lewis Publishers, Boca Raton.

Clayton, J.S., Ehrlich, W.A., Cann, D.B., Day, J.H., Marshall, I.B., 1977. *Soils of Canada*. Vol. 1. Soil Report. Research Branch. Canada Department of Agriculture, Ottawa.

Dokuchaev, V.V., 1892. *Our Steppes — At One Time and Now*. Yevdokimoff Press, St. Petersburg (in Russian).

Evans, I.S., 1980. An integrated system of terrain analysis and slope mapping. *Zeitschrift für Geomorphologie Suppl.* 36, 274–295.

Fedoseev, A.P., 1959. Soil moisture and terrain topography. In: Kon'yukhov, N.A. (Ed.), *Agricultural Meteorology*. Hydrometeorological Press, Moscow (in Russian).

Feranec, J., Kolár, J., Krcho, J., 1991. Mapping of the surface water logging intensity of the soils by applying Landsat TM data and complex digital terrain model. *Bulletin du Comité Français de Cartographie* 127–128, 154–157.

Fitzmaurice, J., Eilers, R.G., St. Jacques, E., Waddell, A., 1999. Soils of SE 32-14-25W — Miniota Precision Agriculture Research Site. Special Report Series 99-1. Land Resource Unit, Agriculture and Agri-Food Canada, Winnipeg.

Florinsky, I.V., 1998. Combined analysis of digital terrain models and remotely sensed data in landscape investigations. *Progress in Physical Geography* 22 (1), 33–60.

Florinsky, I.V., 2000. Relationships between topographically expressed zones of flow accumulation and sites of fault intersection: analysis by means of digital terrain modelling. *Environmental Modelling and Software* 15 (1), 87–100.

Florinsky, I.V., Arlashina, H.A., 1998. Quantitative topographic analysis of gilgai soil morphology. *Geoderma* 82 (4), 359–380.

Florinsky, I.V., Kuryakova, G.A., 1996. Influence of topography on some vegetation cover properties. *Catena* 27 (2), 123–141.

Florinsky, I.V., Kuryakova, G.A., 2000. Determination of grid size for digital terrain modelling in landscape investigations — Exemplified by soil moisture distribution at a micro-scale. *International Journal of Geographical Information Science* 14 (8), 815–832.

Florinsky, I.V., Grokhлина, T.I., Mikhailova, N.L., 1995. LANDLORD 2.0: the software for analysis and mapping of geometrical characteristics of relief. *Geodesiya i Cartographiya* (5), 46–51 (in Russian).

Gerrard, A.J., 1981. *Soils and Landforms. An Integration of Geomorphology and Pedology*. George Allen and Unwin, London.



- Gessler, P.E., Moore, I.D., McKenzie, N.J., Ryan, P.J., 1995. Soil-landscape modelling and spatial prediction of soil attributes. *International Journal of Geographical Information Systems* 9 (4), 421–432.
- Jenny, H., 1961. Derivation of state factor equations of soils and ecosystems. *Soil Science Society of America Proceedings* 25 (5), 385–388.
- Heddadj, D., Gascuel-Oudou, C., 1999. Topographic and seasonal variations of unsaturated hydraulic conductivity as measured by tension disc infiltrometers at the field scale. *European Journal of Soil Science* 50 (2), 275–283.
- Hodgson, M.E., Gaile, G.L., 1996. Characteristic mean and dispersion in surface orientations for a zone. *International Journal of Geographical Information Science* 10 (7), 817–830.
- Huggett, R.J., 1975. Soil landscape systems: a model of soil genesis. *Geoderma* 13 (1), 1–22.
- King, D., Bourennane, H., Isambert, M., Macaire, J.J., 1999. Relationship of the presence of a non-calcareous clay-loam horizon to DEM attributes in a gently sloping area. *Geoderma* 89 (1–2), 95–111.
- Kirkby, M.J., Chorley, R.J., 1967. Throughflow, overland flow and erosion. *Bulletin of the International Association of Scientific Hydrology* 12 (3), 5–21.
- Klute, A. (Ed.), 1986. *Methods of Soil Analysis. Part 1: Physical and Mineralogical Methods*, 2nd ed. Soil Science Society of America, Madison.
- Koshkarev, A.V., 1982. Topography as an input parameter for mathematical and cartographic models of geosystems. In: *Geographical Cartography in Scientific Research and National Economic Practices*. Moscow Branch of the Soviet Geographical Society, Moscow (in Russian).
- Kovda, V.A., 1973. *The Principles of Pedology. General Theory of Soil Formation*, vol. 2. Nauka, Moscow (in Russian).
- Lanyon, L.E., Hall, G.F., 1983. Land surface morphology: 2. Predicting potential landscape instability in eastern Ohio. *Soil Science* 136 (6), 382–386.
- MacMillan, R.A., Pettapiece, W.W., 1997. *Soil Landscape Models: Automated Landscape Characterization and Generation of Soil-Landscape models*. Technical Bulletin No. 1997-1E. Research Branch, Agriculture and Agri-Food Canada, Lethbridge.
- Mardia, K.V., 1972. *Statistics of Directional Data*. Academic Press, London.
- Martz, L.W., De Jong, E., 1988. CATCH: a Fortran program for measuring catchment area from digital elevation models. *Computers and Geosciences* 14 (5), 627–640.
- Moore, I.D., Gessler, P.E., Nielsen, G.A., Peterson, G.A., 1993. Soil attribute prediction using terrain analysis. *Soil Science Society of America Journal* 57 (2), 443–452.
- Moore, I.D., Grayson, R.B., Ladson, A.R., 1991. Digital terrain modelling: a review of hydrological, geomorphological and biological applications. *Hydrological Processes* 5 (1), 3–30.
- Odeh, I.O.A., McBratney, A.B., Chittleborough, D.J., 1994. Spatial prediction of soil properties from landform attributes derived from a digital elevation model. *Geoderma* 63 (3–4), 197–214.
- Page, A.L., Miller, R.H., Keeney, D.R. (Eds.), 1982. *Methods of Soil Analysis. Part 2: Chemical and Microbiological Properties*, 2nd ed. Soil Science Society of America, Madison.
- Parkinson, B.W., Spilker, J.J. (Eds.), 1996. *Global Positioning System: Theory and Applications*. Vols. 1 and 2. American Institute of Aeronautics and Astronautics, Washington.
- Pennock, D.J., Zebarth, B.J., De Jong, E., 1987. Landform classification and soil distribution in hummocky terrain, Saskatchewan, Canada. *Geoderma* 40 (3–4), 297–315.
- Ponagaibo, N.D., 1915. Towards the Influence of Microtopography on Soil Character, its Temperature, Moisture and Productivity. *Reconnaissance Works on Study of Microtopography at the Drabov Test Field Connected with Agricultural Meteorological Observations*. Frishberg Typolithographic Press, Poltava (in Russian).
- Romanova, E.N., 1970. Seasonal humidification of soils in contrast geomorphic conditions. In: Goltsberg, I.A., Romanova, E.N. (Eds.), *Microclimatology*. Hydrometeoizdat, Leningrad (in Russian).
- Romanova, E.N., 1971. Approach of measurement and mapping of soil moisture using morphometric data. In: Goltsberg, I.A., Davitaya, F.F. (Eds.), *Climate of Soil*. Hydrometeoizdat, Leningrad (in Russian).
- Romanova, E.N., 1977. *Microclimatic Variability of the Main Elements of Climate*. Hydrometeoizdat, Leningrad (in Russian, with English abstract).
- Satalkin, A.I., 1996. Development of Automated Technique for Compilation of Middle Scale Soil Maps. Report on Project No. 134. Russian Institute of Monitoring of Lands and Ecosystems, Moscow (unpublished, in Russian).
- Shary, P.A., 1991. The second derivative topographic method. In: Stepanov, I.N. (Ed.), *The Geometry of the Earth Surface Structures*. Pushchino Research Centre Press, Pushchino (in Russian).
- Shary, P.A., 1995. Land surface in gravity points classification by complete system of curvatures. *Mathematical Geology* 27 (3), 373–390.
- Shary, P.A., Kuryakova, G.A., Florinsky, I.V., 1991. On the international experience of topographic methods employment in landscape researches (a concise review). In: Stepanov, I.N. (Ed.), *The Geometry of the Earth Surface Structures*. Pushchino Research Centre Press, Pushchino (in Russian).
- Soil Classification Working Group, 1998. *The Canadian System of Soil Classification*, 3rd ed. NRC Research Press, Ottawa.
- Speight, J.G., 1968. Parametric description of landform. In: Stewart, G.A. (Ed.), *Land Evaluation*. Macmillan, Melbourne.
- Speight, J.G., 1974. A parametric approach to landform regions. In: Brown, E.H., Waters, R.S. (Eds.), *Progress in Geomorphology*. Institute of British Geographers, London.
- Speight, J.G., 1980. The role of topography in controlling throughflow generation: a discussion. *Earth Surface Processes* 5 (2), 187–191.
- Stepanov, I.N., Abdunazarov, U.K., Brynskikh, M.N., Deeva, N.F., Ilyina, A.A., Peido, L.P., Povetukhina, Z.F., Khakimov, F.I., 1984. *Temporal Guide for Compilation of Large- and Middle-Scale Maps of 'Relief Plasticity'*. Biological Research Centre Press, Pushchino (in Russian).
- Stepanov, I.N., Florinsky, I.V., Shary, P.A., 1991. On the conceptual scheme of landscape investigations. In: Stepanov, I.N. (Ed.), *The Geometry of the Earth Surface Structures*. Pushchino Research Centre Press, Pushchino (in Russian).
- Taychinov, S.N., Fayzullin, M.M., 1958. Dynamics of soil moisture in relation to topography. *Soviet Soil Science* (10), 1121–1126.
- Thompson, J.A., Bell, J.C., Butler, C.A., 1997. Quantitative soil-landscape modeling for estimating the areal extent of hydromorphic soils. *Soil Science Society of America Journal* 61 (3), 971–980.
- Walker, P.H., Hall, G.F., Protz, R., 1968. Relation between landform parameters and soil properties. *Soil Science Society of America Proceedings* 32 (1), 101–104.
- Watson, D., 1992. *Contouring: A Guide to the Analysis and Display of Spatial Data*. Pergamon Press, Oxford.
- Weibel, R., Heller, M., 1991. Digital terrain modelling. In: Maguire, D.J., Goodchild, M.F., Rhind, D. (Eds.), *Geographical Information Systems: Principles and Applications*. Vol. 1: Principles. Longman, Harlow.
- Zakharov, S.A., 1940. Importance of slope aspect and gradient for soil and vegetation distribution in the Great Caucasus. *Journal Botanique de l'URSS* 25 (4–5), 378–405 (in Russian).